 CMC, vol.30, no.1, pp.1-18, 2012

3D FEM Analysis of the Buckling Delamination of a Rectangular Viscoelastic Composite Plate with an Embedded Rectangular Crack Under Two-Axial Compression

S. D. Akbarov[1], N. Yahnioglu[2] and E. E. Karatas[2]

Abstract: In Akbarov, Yahnioglu and Karatas (2010) a buckling delamination problem for a rectangular viscoelastic composite plate with a band and edge cracks was investigated under uniaxial compression of the plate. In the present study this investigation is developed for the case where the mentioned rectangular plate contains an embedded rectangular crack and in addition it is assumed that the plate is subjected to two-axial compression.

It is supposed that all end surfaces of the considered plate are simply supported and that these ends are subjected to uniformly distributed normal compressive forces with intensity p_1 and p_3 which act along the Ox_1 and Ox_3 axes, respectively. Moreover, we assume that the plate contains a rectangular embedded crack, the edge-surfaces of which have initial infinitesimal imperfections before the loading.

The evolution of these initial imperfections with time under two-axial compression of the plate is studied within the framework of the three-dimensional geometrically nonlinear field equations of the theory of viscoelasticity for anisotropic bodies.

For determination of the values of the critical force or of the critical time, as well as those of the buckling delamination mode of the considered plate, the initial imperfection criterion is used.

For the solution to the corresponding boundary-value problems, boundary form perturbation techniques; the Laplace transform; the Schapery method for obtaining the numerical inverse Laplace transform of the sought values; and the 3D FEM are used.

The numerical results of the critical force and critical time, as well as of the buckling delamination modes are presented and discussed.

Keywords: Buckling delamination, critical force, critical time, crack, rectangular

[1] YTU, Istanbul, Turkey and Inst.Math.Mech., National Academy of Science of Azerbaijan, Baku, Azerbaijan.

[2] YTU, Istanbul, Turkey.

plate, 3D finite element, viscoelastic composite material

1 Introduction

One of the most common failure mechanisms in laminated composite materials is a local buckling around the delaminated zone, i.e. of the zone in which two adjacent layers are partially debonded with each other at their interface. Note that this zone may be formed as a consequence of various impact events, poor fabrication processes and fatigue. As is well-known, the compressive strength of structures made of unidirectional fibrous-laminated composite materials may be reduced several times by the presence of a damaged bonded zone, which is modeled as a crack in related investigations. A review of these investigations is given in the papers by Hwang and Mao (1999), Short, Guild and Pavier (2001), Arman, Zor and Aksoy (2006) and others in which it is supposed that there is a crack whose edges are parallel to the free plane and to the direction of the compressed external forces. In the foregoing investigations the beginning of the delamination growing process is modeled as a buckling of the part of the material which occupies the region between the crack and the aforementioned free plane. Solutions are found in the framework of the approximate stability loss theories of plates or beams. It is evident that the results of these investigations do not apply in the cases where the thickness of the mentioned part is equal to or greater than the length of the crack. Therefore, it is necessary to develop buckling-failure theories within the framework of the Three Dimensional Linearized Theory of Stability (TDLTS) of deformable solid body mechanics, as carried out by Guz (1990, 1999), Guz and Nazarenko (1989a, 1989b) and others. A review of the related investigations is given in the paper by Guz, Dyshel and Nazarenko (2004). In all the investigations reviewed above, it was assumed that the materials of the composites are time-independent. In the papers by Akbarov (1998, 2007), Akbarov, Sisman and Yahnioglu (1997), Akbarov and Yahnioglu (2001), and Akbarov and Mamedov (2009) the TDLTS is developed for time-dependent materials. The development and application of the above-noted version of the TDLTS on the study of the buckling delamination problems of the elements of construction (such as plate-strips and circular plates) made from viscoelastic materials was done in papers by Akbarov and Rzayev (2002a, 2002b, 2003), Rzayev and Akbarov (2002) and others.

In the paper by Akbarov, Yahnioglu and Karatas (2010) the aforementioned method and investigations were developed for the three-dimensional buckling delamination problem for a rectangular viscoelastic composite plate containing a rectangular band and edge cracks. In the present paper both the method and the investigations carried out in this paper are developed for the three-dimensional buckling delamination problem for a rectangular viscoelastic composite plate containing an

embedded rectangular crack.

Throughout the investigations, the considered composite material is modelled as an orthotropic viscoelastic material with effective mechanical properties. For the solution to the corresponding boundary value problems the boundary form perturbation technique; the Laplace transform; the Schapery method for obtaining the numerical inverse Laplace transform of the sought values; and the 3D FEM are employed.

2 Formulation of the problem

Consider a thick rectangular plate with the geometry shown in Fig 1. The Cartesian coordinate system $Ox_1x_2x_3$ is associated with the plate so as to give Lagrange coordinates of points of the plate. Assume that the plate occupies the region:

$$\left(\Omega - \Omega'\right) \tag{1}$$

where,

$$\Omega = \{0 \le x_1 \le \ell_1,\ 0 \le x_2 \le h,\ 0 \le x_3 \le \ell_3\}$$

$$\Omega' = \{(\ell_1 - \ell_{10})/2 \le x_1 \le (\ell_1 + \ell_{10})/2\,,\ x_2 = h_A \pm 0,\ (\ell_3 - \ell_{30})/2 \le x_3 \le (\ell_3 + \ell_{30})/2\} \tag{2}$$

In Equation (2), $\ell_{10}\,(\ell_{30})$ is the length of the crack along the Ox_1 (Ox_3) axis. It is supposed that the edge surfaces of the crack have insignificant initial imperfections and these imperfections are symmetric with respect to both the $x_1 = \ell_1/2$ and $x_3 = \ell_3/2$ planes. The equations of the crack edge surfaces are given as follows:

$$\begin{aligned} x_2^{\pm} =& h_A + \varepsilon f^{\pm}(x_1, x_3), \\ & (\ell_1 - \ell_{10})/2 \le x_1 \le (\ell_1 + \ell_{10})/2,\ (\ell_3 - \ell_{30})/2 \le x_3 \le (\ell_3 + \ell_{30})/2 \end{aligned} \tag{3}$$

where ε is the dimensionless small parameter ($\varepsilon << 1$) which characterizes the degree of the initial imperfection of the crack's edge surface and the upper symbol "+" ("-'') shows the upper (lower) edge surface of the crack. It is also supposed that the function $f(x_1, x_3)$ and its first order derivatives are satisfied by the following equations:

$$f^{\pm}(\ell_1 - \ell_{01}/2, x_3)\big|_{(\ell_3 - \ell_{30})/2 \le x_3 \le (\ell_3 + \ell_{30})/2} = 0,$$

$$f^{\pm}((\ell_1 + \ell_{10})/2, x_3)\big|_{(\ell_3 - \ell_{30})/2 \le x_3 \le (\ell_3 + \ell_{30})/2} = 0,$$

$$\left.\frac{\partial f^{\pm}((\ell_1-\ell_{10})/2,x_3)}{\partial x_1}\right|_{(\ell_3-\ell_{30})/2\le x_3\le(\ell_3+\ell_{30})/2}=0,$$

$$\left.\frac{\partial f^{\pm}((\ell_1+\ell_{10})/2,x_3)}{\partial x_1}\right|_{(\ell_3-\ell_{30})/2\le x_3\le(\ell_3+\ell_{30})/2}=0,$$

$$f^{\pm}(x_1,(\ell_3-\ell_{30})/2)\big|_{(\ell_1-\ell_{10})/2\le x_1\le(\ell_1+\ell_{10})/2}=0,$$

$$f^{\pm}(x_1,(\ell_3+\ell_{30})/2)\big|_{(\ell_1-\ell_{10})/2\le x_1\le(\ell_1+\ell_{10})/2}=0,$$

$$\left.\frac{\partial f^{\pm}(x_1,(\ell_3-\ell_{30})/2)}{\partial x_3}\right|_{(\ell_1-\ell_{10})/2\le x_1\le(\ell_1+\ell_{10})/2}=0,$$

$$\left.\frac{\partial f^{\pm}(x_1,(\ell_3+\ell_{30})/2)}{\partial x_3}\right|_{(\ell_1-\ell_{10})/2\le x_1\le(\ell_1+\ell_{10})/2}=0. \tag{4}$$

Thus, based on the above, we investigate the evolution of the foregoing initial infinitesimal imperfections of the crack edge surfaces under the action of two-axial compression. This development is investigated by the use of the three-dimensional geometrically nonlinear equations of the theory of viscoelasticity for an anisotropic body. The governing field equations of this theory are:

$$\frac{\partial}{\partial x_j}\left[\sigma_{jn}\left(\delta_i^n+\frac{\partial u_i}{\partial x_n}\right)\right]=0,\quad \sigma_{ij}=C_{ijrs}(0)\,\varepsilon_{rs}(t)+\int_0^t C_{ijrs}(t-\tau)\,\varepsilon_{rs}(\tau)\,d\tau$$

$$\varepsilon_{ij}=\frac{1}{2}\left(\frac{\partial u_i}{\partial x_j}+\frac{\partial u_j}{\partial x_i}+\frac{\partial u_n}{\partial x_i}\frac{\partial u_n}{\partial x_j}\right),\quad i;j;r;s=1,2,3. \tag{5}$$

In equation (5) the conventional notation is used.

For the case under consideration the boundary conditions can be written as follows:

$$u_2|_{x_1=0;\ell_1}=u_2|_{x_3=0,\ell_3}=0$$

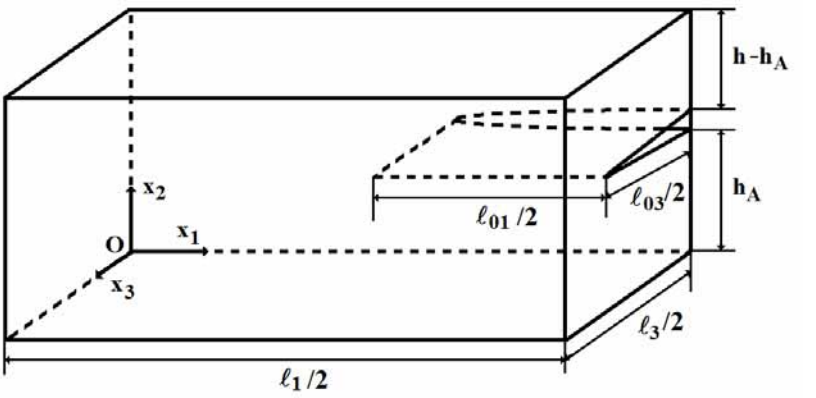

(a)

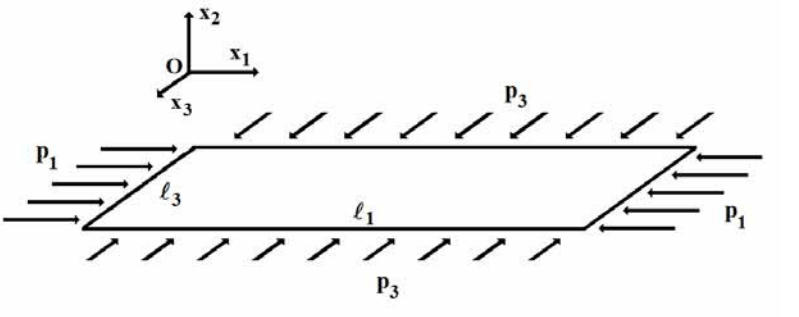

(b)

Figure 1: The geometry of the considered quarter plate with (a) an embedded crack and (b) loading condition.

$$\left[\sigma_{1n}\left(\delta_i^n+\frac{\partial u_i}{\partial x_n}\right)\right]\Big|_{x_1=0;\ell_1}=p_1\delta_i^1,\quad \left[\sigma_{3n}\left(\delta_i^n+\frac{\partial u_i}{\partial x_n}\right)\right]\Big|_{x_3=0;\ell_3}=p_3\delta_i^3$$

$$\left[\sigma_{jn}\left(\delta_i^n+\frac{\partial u_i}{\partial x_n}\right)\right]n_j^{\pm}\Big|_{\substack{x_2^{\pm}=h_A+\varepsilon f^{\pm}(x_1,x_3)\\ (\ell_1-\ell_{10})/2\le x_1\le(\ell_1+\ell_{10})/2\\ (\ell_3-\ell_{30})/2\le x_3\le(\ell_3+\ell_{30})/2}}=0,\quad i;j;n=1,2,3 \tag{6}$$

where n_j ($n_j^{\pm}$) is the orthonormal component of the unit normal vector of the considered surfaces (i.e. the crack edge surfaces).

This completes the formulation of the problem.

3 Method of solution

According to Akbarov (1998), Akbarov and Yahnioglu (2001), Akbarov, Sisman and Yahnioglu (1997), and Akbarov and Rzayev (2002a, 2002b, 2003), the sought values are represented in series form in terms of ε as follows:

$$\left\{\sigma_{ij};\varepsilon_{ij};u_i\right\}=\sum_{q=0}^{\infty}\varepsilon^q\left\{\sigma_{ij}^{(q)};\varepsilon_{ij}^{(q)};u_i^{(q)}\right\} \tag{7}$$

Employing the solution procedure developed in the paper by Akbarov, Yahnioglu and Karatas (2010) we obtain the closed system of equations and boundary conditions for each approximation in (7). As was noted in Akbarov, Yahnioglu and Karatas (2010) and others, for determination of the values of the critical parameters we use the zeroth and first approximations only. Under the aforementioned solution procedure it is assumed that $\delta_i^n+\frac{\partial u_i^{(0)}}{\partial x_n}\approx\delta_i^n$. According to this and to the corresponding boundary conditions for the zeroth approximation, we obtain:

$$\sigma_{11}^{(0)}=p_1,\ \sigma_{33}^{(0)}=p_3 \text{ and } \sigma_{ij}^{(0)}=0,\quad ij\neq 11,33 \tag{8}$$

Moreover, according to the relation $\delta_i^n+\partial u_i^{(0)}/\partial x_n\approx\delta_i^n$, and expression (8) we obtain the following equations and boundary conditions for the first approximation:

$$\frac{\partial}{\partial x_j}\left[\sigma_{ji}^{(1)}+\sigma_{jn}^{(0)}\frac{\partial u_i^{(1)}}{\partial x_n}\right]=0,\quad \varepsilon_{ij}^{(1)}=\frac{1}{2}\left(\frac{\partial u_i^{(1)}}{\partial x_j}+\frac{\partial u_j^{(1)}}{\partial x_i}\right), \tag{9}$$

$$u_2^{(1)}\Big|_{x_1=0;\ell_1}=0,\quad u_2^{(1)}\Big|_{x_3=0;\ell_3}=0,$$

$$\left[\sigma_{11}^{(1)}+\sigma_{11}^{(0)}\frac{\partial u_1^{(1)}}{\partial x_1}\right]\Bigg|_{x_1=0;\ell_1}=0,\ \sigma_{13}^{(1)}|_{x_1=0;\ell_1}=0$$

$$\sigma_{31}^{(1)}\Big|_{x_3=0;\ell_3}=0,\ \left[\sigma_{33}^{(1)}+\sigma_{33}^{(0)}\frac{\partial u_3^{(1)}}{\partial x_3}\right]\Bigg|_{x_3=0;\ell_3}=0,\quad \sigma_{2i}^{(1)}\Big|_{x_2=0;h}=0,\quad i=1,2,3 \tag{10}$$

$$\sigma_{2i}^{(1)}\Big|_{\substack{x_2^{\pm}=h_A\pm 0\\ (\ell_1-\ell_{10})/2\le x_1\le(\ell_1+\ell_{10})/2\\ (\ell_3-\ell_{30})/2\le x_3\le(\ell_3+\ell_{30})/2}} = \pm\sigma_{11}^{(0)}\frac{\partial f^{\pm}}{\partial x_1}\delta_i^1 \pm \sigma_{33}^{(0)}\frac{\partial f^{\pm}}{\partial x_3}\delta_i^3,$$

$$i=1,2,3. \quad (11)$$

Note that the equations (9) and the conditions (10) and (11) are obtained from equation (5) (except the constitutive relations) and from the conditions (6) respectively.

Let us assume that the material of the considered plate is homogeneous and transversally isotropic with the principle axis of elastic symmetries Ox_1,Ox_2 and Ox_3. In this case, the constitutive relations of the plate material can be written as follows:

$$\sigma_{ii}^{(q)} = A_{ij}\varepsilon_{jj}^{(q)}, \quad i;j=1,2,3,$$

$$\sigma_{12}^{(q)} = 2A_{66}\varepsilon_{12}^{(q)}, \quad \sigma_{13}^{(q)} = 2A_{55}\varepsilon_{13}^{(q)},$$

$$\sigma_{23}^{(q)} = 2A_{44}\varepsilon_{23}^{(q)}, \quad q=0,1,2,\ldots \quad (12)$$

In Eq. (12) $A_{11},\ldots,A_{66}$ are the following operators:

$$A_{ij}\varphi(t) = A_{ij0}\varphi(t) + \int_0^t A_{ij1}(t-\tau)\varphi(\tau)d\tau, \quad ij=11;22;33;12;13;23;44;55;66 \quad (13)$$

The meaning of the notation used in Eqs. (12) and (13) is obvious.

Thus, the investigation of the buckling delamination around a rectangular edge crack contained within a thick rectangular plate is reduced to the solutions of series-boundary value problems such as (9)-(13). As in papers by Akbarov and Rzayev (2002a, 2002b, 2003) and others, by direct verification it is proven that the linear equations in (9)-(13) coincide with the corresponding equations for the TDLTS which are presented by Guz (1990, 1999).

Hence for the investigation of the buckling delamination of the plate under consideration we must solve the boundary value problem (9)-(12). For this purpose we use the principle of correspondence by using the Laplace transform:

$$\bar{\varphi}(s) = \int_0^{\infty}\varphi(t)e^{-st}dt \quad (14)$$

with the parameter $s>0$ to the equations (9)-(13). So, replacing $\sigma_{ij}^{(1)}$, $\varepsilon_{ij}^{(1)}$, $u_i^{(1)}$ and A_{ij} in (9)-(13) by $\bar{\sigma}_{ij}^{(1)}$, $\bar{\varepsilon}_{ij}^{(1)}$, $\bar{u}_i^{(1)}$ and $\bar{A}_{ij}$ respectively, we obtain the corresponding

equations and boundary conditions with respect to the Laplace transform of values for the first approximation. For the solution to the considered problem we employ the FEM and for the FEM modeling of the problem we use the functional:

$$\Pi = \frac{1}{2}\iiint\limits_{\Omega-\Omega'}\left[\left(\bar{\sigma}_{11}^{(1)}+\sigma_{11}^{(0)}\frac{\partial\bar{u}_1^{(1)}}{\partial x_1}+\sigma_{33}^{(0)}\frac{\partial\bar{u}_1^{(1)}}{\partial x_3}\right)\frac{\partial\bar{u}_1^{(1)}}{\partial x_1}+\bar{\sigma}_{12}^{(1)}\frac{\partial\bar{u}_1^{(1)}}{\partial x_2}+\bar{\sigma}_{13}^{(1)}\frac{\partial\bar{u}_1^{(1)}}{\partial x_3}+\right.$$
$$\left(\bar{\sigma}_{21}^{(1)}+\sigma_{11}^{(0)}\frac{\partial\bar{u}_1^{(1)}}{\partial x_1}+\sigma_{33}^{(0)}\frac{\partial\bar{u}_1^{(1)}}{\partial x_3}\right)\frac{\partial\bar{u}_2^{(1)}}{\partial x_1}+\bar{\sigma}_{22}^{(1)}\frac{\partial\bar{u}_2^{(1)}}{\partial x_2}+\bar{\sigma}_{23}^{(1)}\frac{\partial\bar{u}_2^{(1)}}{\partial x_3}+$$
$$\left.\left(\bar{\sigma}_{31}^{(1)}+\sigma_{11}^{(0)}\frac{\partial\bar{u}_3^{(1)}}{\partial x_1}+\sigma_{33}^{(0)}\frac{\partial\bar{u}_3^{(1)}}{\partial x_3}\right)\frac{\partial\bar{u}_3^{(1)}}{\partial x_1}+\bar{\sigma}_{32}^{(1)}\frac{\partial\bar{u}_3^{(1)}}{\partial x_2}+\bar{\sigma}_{33}^{(1)}\frac{\partial\bar{u}_3^{(1)}}{\partial x_3}\right]dx_1dx_2dx_3-$$
$$\int\limits_{(\ell_3-\ell_{30})/2}^{(\ell_3+\ell_{30})/2}\int\limits_{(\ell_1-\ell_{10})/2}^{(\ell_1+\ell_{10})/2}\frac{1}{s}\sigma_{11}^{(0)}\frac{\partial f^-}{\partial x_1}\bar{u}_1^{(1)}\Big|_{x_2=h_A-0}dx_1dx_3-$$
$$\int\limits_{(\ell_3-\ell_{30})/2}^{(\ell_3+\ell_{30})/2}\int\limits_{(\ell_1-\ell_{10})/2}^{(\ell_1+\ell_{10})/2}\frac{1}{s}\sigma_{11}^{(0)}\frac{\partial f^+}{\partial x_1}\bar{u}_1^{(1)}\Big|_{x_2=h_A+0}dx_1dx_3-$$
$$\int\limits_{(\ell_3-\ell_{30})/2}^{(\ell_3+\ell_{30})/2}\int\limits_{(\ell_1-\ell_{10})/2}^{(\ell_1+\ell_{10})/2}\frac{1}{s}\sigma_{33}^{(0)}\frac{\partial f^+}{\partial x_3}\bar{u}_3^{(1)}\Big|_{x_2=h_A-0}dx_1dx_3-$$
$$\int\limits_{(\ell_3-\ell_{30})/2}^{(\ell_3+\ell_{30})/2}\int\limits_{(\ell_1-\ell_{10})/2}^{(\ell_1+\ell_{10})/2}\frac{1}{s}\sigma_{33}^{(0)}\frac{\partial f^+}{\partial x_3}\bar{u}_3^{(1)}\Big|_{x_2=h_A+0}dx_1dx_3 \quad (15)$$

For the numerical investigations, the solution domain is divided into a finite number of standard rectangular prism (brick) finite elements with eight nodes. The number of finite elements is determined from the convergence requirement of the numerical results. We should note that all computer programs used in the numerical investigations carried out have been composed by the authors in the package FTN77. After determination of the Laplace transform of the sought values the originals are determined by employing the Schapery method (Schapery (1966)).

4 Numerical results and discussion

We assume that the plate material consists of two alternating layers whose materials are isotropic and homogeneous and that these layers are located in the Ox_1x_3 plane. The reinforcing layers are supposed to be pure elastic with mechanical characteristics $E^{(2)}$ (Young's modulus) and $\nu^{(2)}$ (Poisson coefficient). The material of

the matrix layers is supposed to be linearly viscoelastic with the operators:

$$\mathrm{E}^{(1)} = \mathrm{E}_0^{(1)} \left[1 - \omega_0 R_\alpha^* \left(-\omega_0 - \omega_\infty\right)\right], \quad \nu^{(1)} = \nu_0^{(1)} \left[1 + \frac{1-2\nu_{10}}{2\nu_{10}} \omega_0 R_\alpha^* \left(-\omega_0 - \omega_\infty\right)\right] \tag{16}$$

where $E_0^{(1)}$ are $\nu_0^{(1)}$ are the instantaneous values of Young's modulus and Poisson coefficient, respectively; α, ω_0 and ω_∞ are the rheological parameters of the matrix material, R_α^* is the fractional-exponential operator of Rabotnov (1977) and this operator is determined as:

$$R_\alpha^* \phi(t) = \int_0^t R_\alpha(\beta, t-\tau)\, \phi(\tau)\, dt \tag{17}$$

where

$$R_\alpha(\beta, t) = t^\alpha \sum_{n=0}^{\infty} \frac{\beta^n t^{n(1+\alpha)}}{\Gamma\left((1+n)(1+\alpha)\right)}, \quad -1 < \alpha \le 0 \tag{18}$$

In Eq. (18), $\Gamma(x)$ is the Gamma function.

We introduce the dimensionless rheological parameter $\omega = \omega_\infty / \omega_0$ and the dimensionless time $t' = \omega_0^{1/(1+\alpha)} t$ and assume that $\eta^{(2)} = 0.5$ where $\eta^{(2)}$ is the filler concentration. It is known that in the continuum approach this composite material is taken as a viscoelastic and transversally isotropic material with effective mechanical properties whose isotropy axis lies on the Ox_2 axis. It is known that these effective mechanical properties are determined through the well-known operations described, for example, in the monograph by Christensen (1979).

For the concrete numerical investigations the initial imperfection mode is selected as

$$f^{\pm}(x_1, x_3) = h_A \pm A \sin^2\left(\frac{\pi}{\ell_{10}}\left(x_1 - \frac{\ell_1 - \ell_{10}}{2}\right)\right) \sin^2\left(\frac{\pi}{\ell_{30}}\left(x_3 - \frac{(\ell_3 - \ell_{30})}{2}\right)\right). \tag{19}$$

Thus, we turn to the analysis of the numerical results and at first we consider a pure elastic stability loss buckling delamination which takes place at $t' = 0$ and $t' = \infty$. Note that in all numerical calculations $p_3 = \delta p_1$, $0 \le \delta \le 1$. Hence, the critical values of the external compressive forces which act along the Ox_1 axis denoted by $P_{1cr.0}/E_0^{(1)}$ (for $t' = 0$) and $P_{cr1.\infty}/E_0^{(1)}$ (for $t' = \infty$) are obtained for various δ and

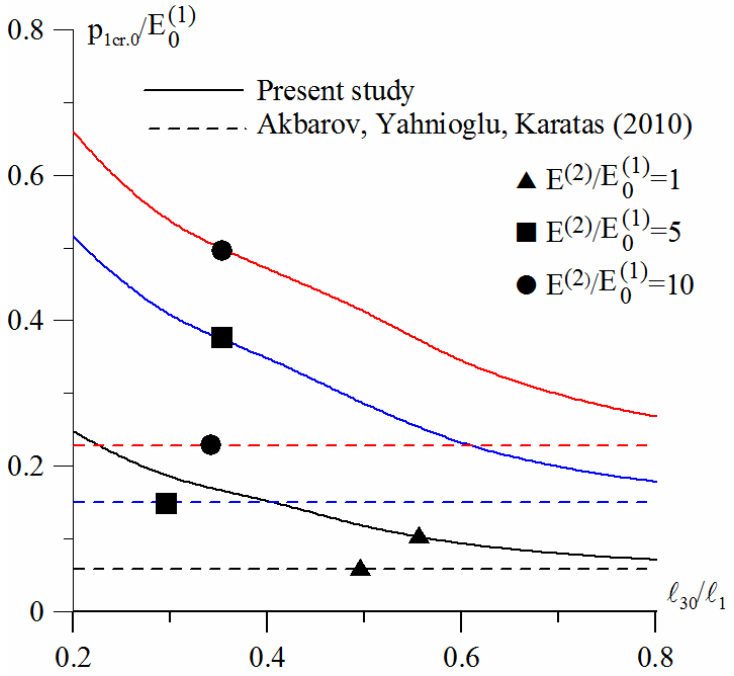

Figure 2: The values of $P_{1cr.0}/E_0^{(1)}$ for various $E^{(2)}/E_0^{(1)}$ and ℓ_{30}/ℓ_1 for which $h/\ell_1 = 0.15$, $\ell_{10}/\ell_1 = 0.5$, $h_A = h/2$, $t' = 0$ and $\omega = 1$

for selected values of the problem parameters. In the present paper, we assume that $h/\ell = 0.15$, $\ell_3/\ell_1 = \gamma_{31} = 1$ and $\nu_0^{(1)} = \nu^{(2)} = 0.3$.

Before analyzing the numerical results, we consider the testing of the algorithm and programs used in obtaining these results. For this purpose we consider the graphs given in Fig. 2 which show the dependence between $P_{1cr.0}/E_0^{(1)}$ and ℓ_{30}/ℓ_1 for various values of $E^{(2)}/E_0^{(1)}$ in the case where $\ell_{10}/\ell_1 = 0.5$ and $h_A = h/2$. In this figure the corresponding values of $P_{1cr.0}/E_0^{(1)}$, obtained in the paper by Akbarov, Yahnioglu and Karatas (2010), are also indicated by dashed lines. According to the well-known mechanical consideration, with ℓ_{30}/ℓ_1 the values of $P_{cr1.0}/E_0^{(1)}$ obtained for an embedded crack must approach the corresponding ones obtained for a band crack. This prediction is proven by the results illustrated in Fig. 2 and this also validates the algorithm and programs used for the present investigation.

Thus, we consider the data given in Table 1 which shows the ratio $\left(P_{1cr.0}/E_0^{(1)}\right)/\left(P_{1cr.\infty}/E_0^{(1)}\right)$ under $\omega = 1$ and $\ell_{30}/\ell_1 = 0.5$ for various of ℓ_{10}/ℓ_1.

It follows from this table that the values of $P_{1cr.0}/E_0^{(1)}$ (given in the numerator of the ratio) and $P_{1cr.\infty}/E_0^{(1)}$ (given in the denominator of the ratio) decrease monotonically with ℓ_{10}/ℓ_1. Moreover the data given in this table show that the bi-axiality of the external compression, i.e. an increase of the ratio $\delta\,(=p_3/p_1)$ causes a decrease in the values of $P_{1cr.0}/E_0^{(1)}$ and $P_{1cr.\infty}/E_0^{(1)}$.

Table 1: The values of $P_{1cr.0}/E_0^{(1)}$($P_{1cr.\infty}/E_0^{(1)}$) in the numerator (denominator) of the ratio for various elasticity modulus ($\mathrm{E}^{(2)}/\mathrm{E}_0^{(1)}$), $\delta = p_3/p_1$ and ℓ_{10}/ℓ_1 under $\ell_{30}/\ell_1 = 0.5$ and $h_A = h/2$

$\mathrm{E}^{(2)}/\mathrm{E}_0^{(1)}$	$\delta = \frac{p_3}{p_1}$	ℓ_{10}/ℓ_1					
		0.6	0.5	0.4	0.3	0.2	0.15
1	0.0	0.1167 0.0858	0.1174 0.0865	0.1203 0.0882	0.1342 0.0971	0.1699 0.1205	0.2021 0.1411
	0.3	0.0933 0.0691	0.0955 0.0705	0.1032 0.0757	0.1220 0.0884	0.1623 0.1151	0.1965 0.1373
	0.5	0.0796 0.0590	0.0838 0.0619	0.0938 0.0688	0.1148 0.0832	0.1573 0.1117	0.1929 0.1348
	1.0	0.0569 0.0422	0.0634 0.0468	0.0756 0.0555	0.0991 0.0719	0.1451 0.1031	0.1829 0.1281
5	0.0	0.2817 0.1966	0.2857 0.2026	0.2884 0.2033	0.3092 0.2091	0.3657 0.2308	0.4146 0.2500
	0.3	0.2313 0.1699	0.2347 0.1706	0.2482 0.1759	0.2815 0.1907	0.3493 0.2207	0.4035 0.2436
	0.5	0.1980 0.1463	0.2063 0.1503	0.2257 0.1601	0.2648 0.1796	0.3387 0.2142	0.3961 0.2393
	1.0	0.1418 0.1048	0.1561 0.1138	0.1819 0.1292	0.2287 0.1555	0.3127 0.1985	0.3766 0.2284
10	0.0	0.4015 0.2537	0.4123 0.2617	0.4135 0.2669	0.4280 0.2677	0.4767 0.2784	0.5196 0.2906
	0.3	0.3436 0.2335	0.3456 0.2341	0.3578 0.2360	0.3903 0.2452	0.4558 0.2666	0.5060 0.2834
	0.5	0.2956 0.2049	0.3046 0.2076	0.3256 0.2153	0.3674 0.2311	0.4422 0.2590	0.4970 0.2787
	1.0	0.2119 0.1470	0.2306 0.1573	0.2627 0.1740	0.3176 0.2004	0.4089 0.2405	0.4733 0.2664

Table 2 shows the influence of ℓ_{30}/ℓ_1 on the values of $P_{1cr.0}/E_0^{(1)}$ (upper number) and $P_{1cr.\infty}/E_0^{(1)}$ (lower number) under $\omega = 1$ and $\ell_{10}/\ell_1 = 0.5$. It follows from this

table that the values of $P_{1cr.0}/E_0^{(1)}$and $P_{1cr.\infty}/E_0^{(1)}$ increase with decreasing crack length in the direction of the Ox_3 axis.

Table 2: The values of $P_{1cr.0}/E_0^{(1)}(P_{1cr.\infty}/E_0^{(1)})$ in the numerator (denominator) of the ratio for various elasticity modulus ($E^{(2)}/E_0^{(1)}$), $\delta = p_3/p_1$ and ℓ_{30}/ℓ_1 under $\ell_{10}/\ell_1 = 0.5$ and $h_A = h/2$

$E^{(2)}/E_0^{(1)}$	$\delta = \frac{p_3}{p_1}$	ℓ_{30}/ℓ_1						
		0.8	0.7	0.6	0.5	0.4	0.3	0.2
1	0.0	0.0713	0.0796	0.0934	0.1174	0.1519	0.1852	0.2480
		0.0529	0.0590	0.0692	0.0865	0.1099	0.1323	0.1747
	0.3	0.0643	0.0699	0.0792	0.0955	0.1252	0.1686	0.2219
		0.0497	0.0518	0.0586	0.0705	0.0918	0.1209	0.1571
	0.5	0.0602	0.0644	0.0714	0.0838	0.1067	0.1490	0.2043
		0.0446	0.0478	0.0529	0.0619	0.0783	0.1079	0.1446
	1.0	0.0515	0.0534	0.0569	0.0634	0.0756	0.0991	0.1451
		0.0383	0.0396	0.0422	0.0468	0.0555	0.0719	0.1031
5	0.0	0.1786	0.1991	0.2321	0.2857	0.3482	0.4079	0.5157
		0.1327	0.1476	0.1705	0.2026	0.2291	0.2606	0.3438
	0.3	0.1609	0.1749	0.1970	0.2347	0.2989	0.3759	0.4724
		0.1197	0.1298	0.1454	0.1706	0.2087	0.2420	0.3027
	0.5	0.1508	0.1612	0.1779	0.2063	0.2564	0.3412	0.4364
		0.1121	0.1197	0.1314	0.1503	0.1820	0.2269	0.2716
	1.0	0.1292	0.1338	0.1418	0.1561	0.1819	0.2287	0.3127
		0.0962	0.0995	0.1048	0.1138	0.1292	0.1555	0.1985
10	0.0	0.2682	0.2986	0.3451	0.4123	0.4715	0.5368	0.6600
		0.1874	0.2077	0.2356	0.2617	0.2817	0.3114	0.4103
	0.3	0.2420	0.2626	0.2942	0.3456	0.4253	0.4990	0.6001
		0.1693	0.1832	0.2035	0.2341	0.2666	0.2934	0.3545
	0.5	0.2266	0.2421	0.2658	0.3046	0.3695	0.4658	0.5609
		0.1586	0.1691	0.1842	0.2076	0.2437	0.2791	0.3261
	1.0	0.1943	0.2010	0.2119	0.2306	0.2627	0.3176	0.4089
		0.1363	0.1406	0.1470	0.1573	0.1740	0.2004	0.2406

Table 3 shows the influence of the distance $(h-h_A)/\ell_1$ between the crack's location plane and the upper face-plane of the plate on the values of $\left(P_{1cr.0}/E_0^{(1)}\right)/\left(P_{1cr.\infty}/E_0^{(1)}\right)$ obtained under $\ell_{10}/\ell_1 = 0.5$ and $\ell_{30}/\ell_1 = 0.5$. This table shows that the values of $P_{1cr.0}/E_0^{(1)}$and $P_{1cr.\infty}/E_0^{(1)}$ decrease rapidly with decreasing $(h-h_A)/\ell_1$.

Table 3: The values of $P_{1cr.0}/E_0^{(1)}$ (numerator) and $P_{1cr.\infty}/E_0^{(1)}$ (denominator) for various$(h-h_A)/\ell_1$, elasticity modulus ($E^{(2)}/E_0^{(1)}$) and $\delta = p_3/p_1$ under $\ell_{10}/\ell_1 = 0.5$ and $\ell_{30}/\ell_1 = 0.5$

$E^{(2)}/E_0^{(1)}$	$\delta = \frac{p_3}{p_1}$	$(h-h_A)/\ell_1$			
		0.0750	0.050	0.0375	0.0250
1	0.0	0.1174 0.0865	0.0579 0.0436	0.0436 0.0329	0.0256 0.0195
	0.1	0.1096 0.0808	0.0533 0.0496	0.0407 0.0308	0.0237 0.0181
	0.5	0.0838 0.0619	0.0398 0.0395	0.0312 0.0237	0.0181 0.0138
	1	0.0634 0.0468	0.0299 0.0302	0.0236 0.0179	0.0136 0.0104
10	0.0	0.4123 0.2617	0.2404 0.1760	0.1808 0.1398	0.1058 0.0874
	0.1	0.3910 0.2557	0.2256 0.2702	0.1701 0.1325	0.0987 0.0818
	0.5	0.3046 0.2076	0.1720 0.1318	0.1326 0.1048	0.0756 0.0631
	1	0.2306 0.1573	0.1648 0.0996	0.1007 0.0798	0.0572 0.0478

Now we consider some numerical results obtained for the critical time i.e. for the t'_{cr}. It is well known that under investigation of the viscoelastic stability loss problem, the selected values of the external force $p_1/E_0^{(1)}$ must satisfy the inequality $P_{1cr.0}/E_0^{(1)} < P_1/E_0^{(1)} < P_{1cr.\infty}/E_0^{(1)}$. For some values of $p_1/E_0^{(1)}$ the results obtained for t'_{cr} are given in Table 4 for various ℓ_{10}/ℓ_1 and $\delta = \frac{p_3}{p_1}$ under $\omega = 1$; $\alpha = -0.5$, $\ell_{30}/\ell_1 = 0.5$ and $E^{(2)}/E_0^{(1)} = 10$. It follows from these results that the values of t'_{cr} decrease with $p_1/E_0^{(1)}$. This statement agrees with obvious mechanical considerations.

Table 5 shows the values of t'_{cr} obtained for various ω and $\delta = p_3/p_1$ under $\alpha = -0.5$, $\ell_{10}/\ell_1 = 0.5$, $\ell_{30}/\ell_1 = 0.5$ and for the selected values of $p_1/E_0^{(1)}$. It follows from these numerical results that the values of t'_{cr} increase with ω . Note that the parameter ω characterizes the modulus of elasticity of the matrix material under $t' = \infty$; therefore the results given in Table 5 confirm known mechanical considerations.

Table 4: The values of t'_{cr} for various $\delta = p_3/p_1$, $\ell_{10}/\ell_1$and $p_1/\mathrm{E}_0^{(1)}$ under $\omega = 1$, $\alpha = -0.5$, $\ell_{30}/\ell_1 = 0.5$ and $\mathrm{E}^{(2)}/\mathrm{E}_0^{(1)} = 10$

$\delta = \frac{p_3}{p_1}$	ℓ_{10}/ℓ_1	$p_1/\mathrm{E}_0^{(1)}$	t'_{cr}
0.3	0.60	0.28	0.4167
		0.30	0.0943
		0.33	0.0042
	0.50	0.28	0.4292
		0.30	0.0994
		0.33	0.0054
	0.40	0.28	0.6187
		0.30	0.1609
		0.33	0.0169
0.5	0.60	0.25	0.2168
		0.27	0.0323
		0.29	0.0009
	0.50	0.25	0.3434
		0.27	0.0629
		0.29	0.0063
	0.40	0.27	0.2033
		0.29	0.0443
		0.32	0.0002

Table 5: The values of t'_{cr} for various $\delta = p_3/p_1$, ω and $p_1/\mathrm{E}_0^{(1)}$ under $\alpha = -0.5$, $\ell_{10}/\ell_1 = 0.5$, $\ell_{30}/\ell_1 = 0.5$ and $\mathrm{E}^{(2)}/\mathrm{E}_0^{(1)} = 10$

$p_1/\mathrm{E}_0^{(1)}$	$\delta = \frac{p_3}{p_1}$	ω	t'_{cr}
0.33	0.3	1	0.0054
		2	0.0067
		3	0.0086
0.27	0.5	1	0.0629
		2	0.1510
		3	0.7446

Table 6 shows the dependencies between α and t'_{cr} for the case where $\omega = 1$, $\ell_{10}/\ell_1 = 0.5$, $\ell_{30}/\ell_1 = 0.5$ and for the selected values of $p_1/\mathrm{E}_0^{(1)}$. From these numerical results it follows that the values of t'_{cr} decrease with $|\alpha|$.

Table 6: The values of t'_{cr} for various $\delta = p_3/p_1$,α and $p_1/\mathrm{E}_0^{(1)}$ under $\omega = 1$, $\ell_{10}/\ell_1 = 0.5$, $\ell_{30}/\ell_1 = 0.5$ and $\mathrm{E}^{(2)}/\mathrm{E}_0^{(1)} = 10$

$p_1/\mathrm{E}_0^{(1)}$	$\delta = \frac{p_3}{p_1}$	α	t'_{cr}
0.33	0.3	-0.3	0.0197
		-0.5	0.0067
		-0.7	0.0002
0.27	0.5	-0.3	0.1137
		-0.5	0.0629
		-0.7	0.0157

Figure 3 shows schematically the distribution of $\frac{u_2 E^{(2)}}{(\ell_1 p_1)}$ with respect x_1 and x_3 under $x_2 = (h - h_A) + 0$ for $\delta = \frac{p_3}{p_1} = 0.3$, $\mathrm{E}^{(2)}/\mathrm{E}_0^{(1)} = 10$, $(h - h_A)/\ell_1 = 0.075$. In other words, Figure 3 shows the buckling delamination mode for the external force $p_1/\mathrm{E}_0^{(1)}$which is very near the corresponding $P_{1cr.0}/E_0^{(1)}$, i.e. $\left| p_{1cr.0}/\mathrm{E}_0^{(1)} - p_1/\mathrm{E}_0^{(1)} \right| \approx 10^{-4}$. Note that in this figure the axis $x_1(\ell_3 - x_3)$ is denoted by x (z). Analysis of the Figure 3 and other related results (which are not illustrated here) shows that in the cases where $\ell_{30} > k.\ell_{10}$ ($k \in R$ and for the considered case k=0.60) the buckling delamination mode is similar (in the geometrical sense) to the initial imperfection mode. However, in the cases where$\ell_{30} \leq 0.60\ell_{10}$ the buckling delamination mode has a more complicated character.

5 Conclusion

According to the foregoing analyses the following main conclusions can be drawn:

1. The type of buckling delamination mode of the embedded rectangular crack surfaces depends not only on the initial imperfection mode, but also on the ratio of the lengths of the rectangular crack along the direction of the Ox_1 and Ox_3 axes,

2. The values of the critical forces decrease monotonically with the crack length along the Ox_1 axis, as well as with the crack depth along the Ox_3axis,

3. The values of the critical forces decrease as the crack gets closer to the free plane of the plate, i.e. with decreasing $(h - h_A)/\ell_1$,

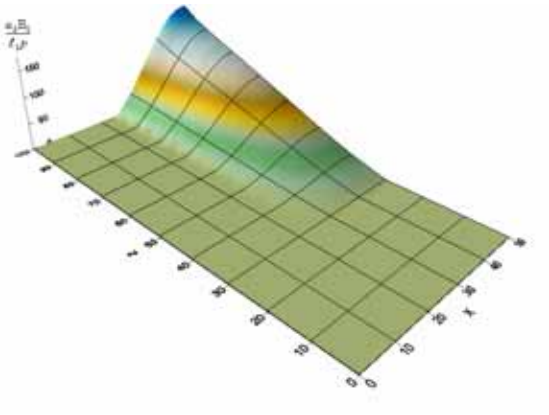

(a)

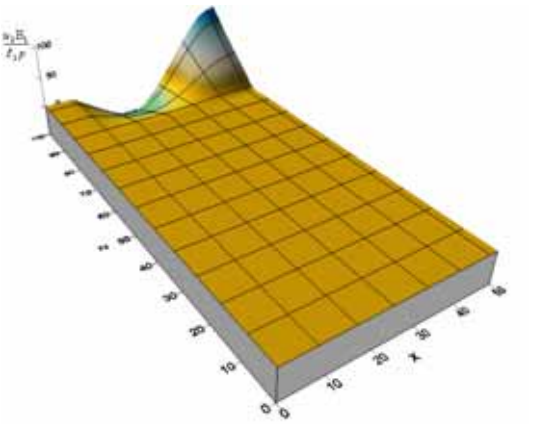

(b)

Figure 3: The buckling delamination mode a) in the case where $\ell_{30} > 0.60\ell_{10}$ and b) in the case where $\ell_{30} \leq 0.60\ell_{10}$

4. The critical time decreases with the $p_1/\mathrm{E}_0^{(1)}$,
5. The values of the critical time (t'_{cr}) increase with rheological parameter ω,
6. For the considered cases the values of the critical time (t'_{cr}) decrease with the absolute values of the rheological parameter α,
7. The two-axiality of the external compressing force, i.e. $\delta = p_3/p_1 \neq 0$ or the

existence of the compressing force p_3 in the Ox_3 axes causes a decrease in the critical value.

References

Akbarov S.D. (1998): On the Three Dimensional Stability Loss Problems of Elements of Constructions Fabricated From the Viscoelastic Composite Materials. *Mechanics of Composite Materials*, vol. 34, no. 6, pp. 537-544.

Akbarov S.D. (2007): Three-dimensional instability problems for viscoelastic composite materials and structural members. *International Applied Mechanics,* vol. 43, no. 10, pp. 1069-1089.

Akbarov S.D.; Mamedov A.R. (2009): On the solution method for problems related to the micro-mechanics of a periodically curved fiber near a convex cylindrical surface. *CMES:Computer Modeling in Engineering&Sciences*, vol. 42, no. 3, pp. 257-296.

Akbarov S.D.; Rzayev O.G. (2002a): Delamination of Unidirectional Viscoelastic Composite Materials., *Mechanics of Composite Materials*, vol. 38, no. 1, pp. 17-24.

Akbarov S.D.; Rzayev O.G. (2002b), On the Buckling of the Elastic and Viscoelastic Composite Circular Thick Plate with a Penny-Shaped Crack. *European Journal of Mechanics A/Solids*, vol. 21, no. 2, pp. 269-279.

Akbarov S.D.; Rzayev O.G. (2003): On the Delamination of a Viscoelastic Composite Circular Plate. *International Applied Mechanics*, vol. 39, no. 3, pp. 368-374.

Akbarov S.D.; Sisman T.; Yahnioglu N. (1997): On the Fracture of the Unidirectional Composites in Compression. *International Journal of Engineering Science*, vol. 35 no. 12/13, pp. 1115-1136.

Akbarov S.D.; Yahnioglu N. (2001): The Method for Investigation of the General Theory of Stability Problems of Structural Elements Fabricated From the Viscoelastic Composite Materials. *Composites Part B: Engineering*, vol. 32, no. 5, pp. 475-482.

Akbarov S. D.; Yahnioglu N.; Karatas E. E. (2010): Buckling delamination of a rectangular plate containing a rectangular crack and made from elastic and viscoelastic composite materials. *International Journal of Solids and Structures*, vol.47, no.25-26, pp.3426-3434.

Arman Y.; Zor M.; Aksoy S. (2006): Determination of Critical Delamination Diameter of Laminated Composite Plates Under Buckling Loads. *Composites Science and Technology*, vol. 66, pp. 2945-2953.

Christensen R.M. (1979): *Mechanics of Composite Materials*. Willey, New York.

Guz A.N. (1990): *Fracture Mechanics of Composite Materials in Compression.* Naukova Dumka, Kiev.

Guz A.N. (1999): *Fundamentals of the Three-Dimensional Theory of Stability of Deformable Bodies'*, Berlin, Springer-Verlag.

Guz A.N.; Dyshel M.N.; Nazarenko V.M. (2004): Fracture and Stability of Materials with Cracks: Approaches and Results. *International Applied Mechanics*, vol. 40, no. 12, pp. 1323-1359.

Guz A.N.; Nazarenko V.M. (1989a): Fracture Mechanics of Materials in Compression Along a Crack, Highly Elastic Materials. *International Applied Mechanics*, vol. 25, no. 9, pp. 3-32.

Guz A.N.; Nazarenko V.M. (1989b): Fracture Mechanics of Materials in Compression Along a Crack Constructional Materials. *International Applied Mechanics*, vol. 25, no. 10, pp. 3-19.

Hwang S.F.; Mao C.P. (1999): The Delamination Buckling of Single-Fibre System and Interply Hybrid Composites. *Composite Structures*, vol. 46, pp. 279-287.

Rabotnov, Yu N. (1977): *Elements of Hereditary Mechanics of Solid Bodies*. Nauka, Moscow (in Russian)

Rzayev O.G.; Akbarov S.D. (2002): Local Buckling of the Elastic and Viscoelastic Coating Around the Penny-Shaped Interface Crack. *International Journal of Engineering Science*, vol. 40, pp. 1435-1451.

Schapery, R.A. (1966): Approximate Methods of Transform Inversion for Viscoelastic Stress Analyses. *Proc. US Nat. Cong. Appl. ASME*, pp. 1075-1085.

Short G.J.; Guild F.J.; Pavier M.J. (2001): The Effect of Delamination Geometry on the Compressive Failure of Composite Laminates. *Composites Science and Technology*, vol. 61, pp. 2075-2086.